IEEJ Journal of Industry Applications
Vol.7 No.5 pp.403–409 DOI: 10.1541/ieejjia.7.403

Paper

Online Degradation Detection/Prediction Method for Current Transfer Ratio of Photo-Coupler Installed in Digitally-Controlled Switching Mode Power Supply

Hiroshi Nakao[*,**a)] Student Member, Yu Yonezawa[*] Member
Takahiko Sugawara[*,***] Non-member, Yoshiyasu Nakashima[*] Member
Fujio Kurokawa[**,****] Senior Member

(Manuscript received June 27, 2017, revised March 12, 2018)

The software-implemented degradation detection/prediction of the current transfer ratio (CTR) of a photo-coupler installed in a digitally-controlled switching mode power supply was studied. The photo-coupler is one of the key devices in an isolated power supply circuit, which transmits a voltage/current signal to a controller though the isolation gap. If the CTR of the photo-coupler degrades to halfway between the normal value and the threshold of the hardware protection circuit, overvoltage/current may be supplied continuously to the load circuit and possibly cause a severe failure. By comparing the theoretical pulse width modulation (PWM) duty, which is calculated from the input/output voltage and the pre-measured power supply circuit efficiency, and the applied PWM duty, which is calculated via feedback control, CTR degradation is detectable online. In this paper, we describe the concept of this method and verify it using both simulation and prototyping circuits.

Keywords: photo-coupler, current transfer ratio, CTR, degradation, failure prediction, digitally-controlled power supply

1. Introduction

The software-implemented degradation detection technique for photo-couplers (PCs) used in an isolated switching mode power supply (SMPS) was studied. The photo-coupler is one of the key devices in an isolated power supply circuit; it is installed in a feedback loop or failure detection circuit and transmits voltage/current signals for control though an isolation gap (Fig. 1). The photo-coupler is also known as one of the life-limited devices in power supply circuits as well as electrolytic capacitors, cooling fans, and so on. Although the average life expectancy of the photo-coupler is much longer than that of the other devices [1], the degradation of the photo-coupler generates a more severe risk, including smoking, ignition or breakage of the power supply or a connected load. Photo-coupler degradation occurs as its gain or current transfer ratio (CTR) decreases and it causes over-voltage and/or over-current of the power supply output.

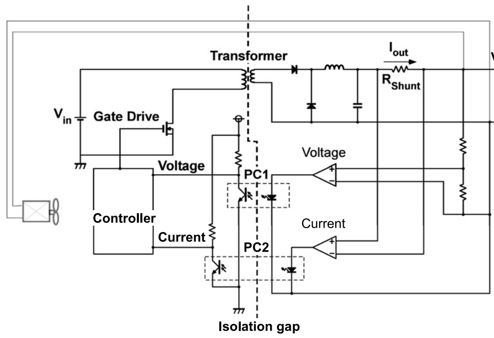

Fig. 1. Schematic diagram of isolated DC-DC converter. Optional cooling fan is plotted with gray line

There are many solutions to compensate for this photo-coupler gain degradation: installing multi photo-couplers for feedback loop and over-voltage protection respectively [2], self-compensation using a photo-coupler IC containing one LED and two closely-matched photodetector pairs [3], digital transmission using a set of DA/AD convertors and a photo-coupler [4], and so on. However, these solutions require additional parts or high-functional ICs and do not fall within the cost and space budget for commercial SMPS. In small size converters particularly, such as 1/16 brick DC-DC [5], the space budget for the isolation gap around the photo-coupler is very severe; in the case of the creeping distance for 8 mm isolation [6], around 5% of the space budget is required for just one photo-coupler.

a) Correspondence to: Hiroshi Nakao. e-mail: nakao.h@jp.fujitsu.com
* Fujitsu laboratories LTD.
1-1, Kamikodanaka 4-choume, Nakahara-ku, Kawasaki 211-8588, Japan
** Nagasaki University
1-14, Bunkyo-machi, Nagasaki, Nagasaki 852-8521, Japan
*** Transtron Inc. Fujisawa Office, Isuzu Motors Shonan R&D Center
2023-18, Endo, Fujisawa 252-0816, Japan
**** Nagasaki Institute of Applied Science, the Division of Electrical, Electronic, and Information Technology
Nagasaki-shi 851-0193, Japan

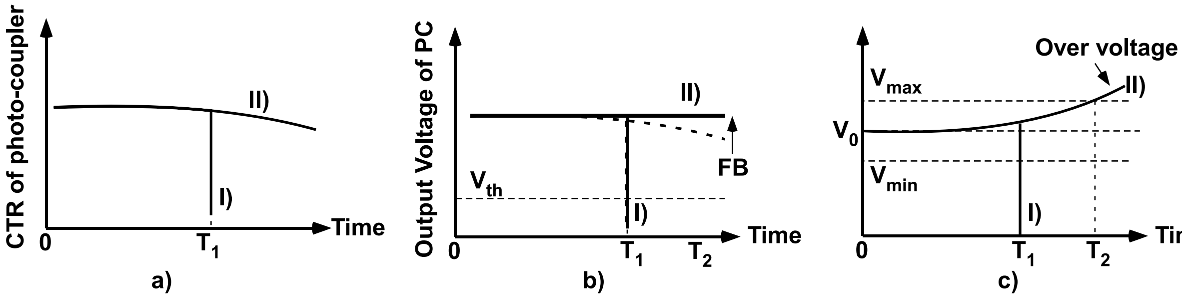

Fig. 2. Schematic mechanism of over-voltage caused by PC CTR degradation. The gradual degradation (noted as II) is more difficult to detect than abrupt degradation (noted as I) and can sometimes cause more severe damage for the connected load

Some controller ICs have a safety circuit which can detect only open or short failures of the photo-coupler signal by detecting an abnormal state[7]. They are cost-effective but cannot detect a gradual degradation of photo-coupler CTR. If the CTR of the photo-coupler degraded to halfway between the normal value and the threshold for failure detection, over-voltage/current may be supplied continuously to the load circuit and possibly cause a severe failure.

We are now proposing a model-based developing (MBD) system[8]–[10] for digitally-controlled SMPS[11][12] and have demonstrated the failure prediction of the output capacitors of the digitally-controlled SMPS based on the MBD scheme[13]–[15]. MBD is a development scheme based on the step-by-step repetition between simulation and verification. This scheme makes it very easy to add a new software-implemented function to the digitally-controlled SMPS. In a digitally-controlled SMPS, the micro-processing unit or MPU controls switching timing with reference to the IV characteristics of power supply circuits instead of analog controller ICs.

If the photo-coupler gain degradation detection is available only from the MPU monitoring data, we can ensure a software-implemented, cost- and space-effective failure prediction method. A protection circuit should probably be included as hardware; however, adding software-implemented protection with a hardware protection circuit means increasing the diversity inherent in its functional safety. Moreover, failure prediction enables a reduction in maintenance costs by enhancing the effectiveness of scheduled preventive maintenance.

In this paper, we propose a new CTR degradation detection/prediction technique for photo-couplers installed in feedback loops and/or current monitoring circuits of digitally-controlled SMPS. First, we briefly describe the concept of this method, followed by prototyping of the control algorithm with model in the loop simulation (MILS), and experimental verification with our original rapid control prototyping (RCP) system. After presenting the results and discussion, we offer a summary.

2. Concept

2.1 Degradation of Photo-coupler CTR Figure 2 shows the mechanism of over voltage caused by photo-coupler CTR degradation: a) degradation mode of CTR, b) output voltage of photo-coupler signal, c) output voltage of SMPS. In these figures, notation I shows an abruptfailure such as a line break or shortage, and notation II shows a gradual degradation such as an ageing effect. In Fig. 2b), dashed and solid lines show open and closed loop characteristics respectively. If the output signal of the photo-coupler shows an abrupt drop (Fig. 2b), line I) caused by an abrupt failure, the output signal of the photo-coupler is not recovered with feedback control and rapidly exceeds the failure detection threshold V_{th}. The controller can easily detect this abnormal state and stop switching for load protection. However, if the CTR of the photo-coupler degrades gradually (Fig. 2a), line II), the feedback loop tries to keep the output voltage of the photo-coupler constant (Fig. 2b), line II) by making the real output voltage higher (Fig. 2c), line II). Finally, the output voltage V_{out} goes up over the voltage limit. In this case, the over-voltage and/or current are continuously applied without fuses blowing and this may cause severe damage including smoking, ignition or breakage of the power supply or the connected load. Under-voltage may occur via the same mechanism; however, CTR increase is difficult to engender. So, in this paper, we will discuss CTR degradation as CTR decrease.

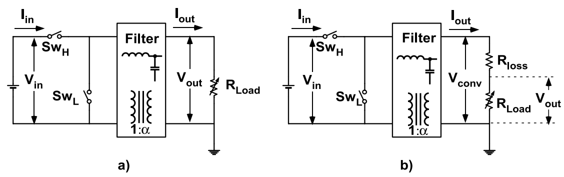

Fig. 3. Schematic relationship between a step-down ratio and an effective resistance

2.2 The New Degradation Detection/Prediction Concept based on Applied Duty Monitoring Figure 3 gives a brief outline of the new photo-coupler degradation detection/prediction method. Figure 3a) is an equivalent forward converter circuit to that shown in Fig. 1, in which some components such as the transformer Tr, inductor L, and capacitor C are summarized as a filter box. The feedback loop controls V_{out} to be constant. If all components of this converter are ideal, that means no loss, and a theoretical duty ratio in steady state D_{tideal} is shown as

$$D_{tideal} = \frac{V_{out}}{\alpha \cdot V_{in}} \qquad (1)$$

where α is a winding ratio of the transformer (Fig. 3a)).

If the components are not ideal (Fig. 3b)), a theoretical duty ratio with loss D_{tloss} is shown as

$$D_{tloss} = \frac{V_{conv}}{\alpha \cdot V_{in}} \cdots\cdots (2)$$

where

$$V_{conv} = V_{out} + R_{loss}(I_{out}) \cdot I_{out} = (R_{load}(I_{out}) + R_{loss}(I_{out})) \cdot I_{out} \cdots\cdots (3)$$

and

$$R_{loss}(I_{out}) = \frac{(V_{in} \cdot I_{in} - V_{out} \cdot I_{out})}{I_{out}^2}. \cdots\cdots (4)$$

$R_{loss}(I_{out})$ is an equivalent resistance (16) which is a virtual resistance assuming the total loss of the converter as resistive and related to output current I_{out}. $R_{loss}(I_{out})$ is dependent on many parameters such as V_{in}, V_{out}, I_{out}, power consumptions of the controller, FET drivers, and so on. However, it can be measured and tabled as a function of I_{out} in firmware for the digitally-controlled SMPS, in advance with practical use of the converter.

Using this equivalent resistance, converter efficiency $\varepsilon(I_{out})$ is shown as

$$\varepsilon(I_{out}) = \frac{V_{out} \cdot I_{out}}{V_{out} \cdot I_{out} + R_{loss}(I_{out}) \cdot I_{out}^2} = \frac{R_{load}(I_{out}) \cdot I_{out}^2}{R_{load}(I_{out}) \cdot I_{out}^2 + R_{loss}(I_{out}) \cdot I_{out}^2} = \frac{R_{load}(I_{out})}{R_{load}(I_{out}) + R_{loss}(I_{out})}. \cdots\cdots (5)$$

Formula (5) shows, converter efficiency $\varepsilon(I_{out})$ can be determined from pre-implemented $R_{loss}(I_{out})$ look-up table and $R_{load}(I_{out})$. When SMPS is normal, V_{out} is constant and equal to designed value, so $R_{load}(I_{out})$. can be determined by MPU fetched I_{out} and target output voltage.

From formula (2) and (5), D_{tloss} is shown as

$$D_{tloss} = \frac{1}{\varepsilon(I_{out})} \cdot \frac{V_{out}}{\alpha \cdot V_{in}} = \frac{1}{\varepsilon(I_{out})} \cdot D_{tideal}. \cdots\cdots (6)$$

This formula means D_{tloss} is estimated from D_{tideal} and efficiency ε at a certain output current I_{out} in steady state. In the initial state of the SMPS, D_{tloss} should be equal to the actual duty ratio $D_{applied}$.

If the CTR of the photo-coupler is degraded, there is a difference between the duty ratio after the degraded $D_{degraded}$ and the theoretical duty ratio D_{tloss}. Comparing the actual applied duty $D_{applied}$, which is calibrated to equal D_{tloss} in advance with practical use of the converter, and $D_{degraded}$, we tried to detect CTR degradation.

First, CTR degradation detection/prediction for the photo-coupler installed in the voltage regulation feedback loop is considered. If the relative CTR of the photo-coupler degrades from 1 to β ($0 < \beta < 1$), the actual V_{out} increases from V_{out} to V_{out}/β. So, applied duty after the degraded D_{PC_V} is formulated as

$$D_{PC\_V} = \frac{1}{\varepsilon(I_{out})} \cdot \frac{V_{out}}{\alpha\beta \cdot V_{in}} = \frac{1}{\beta} \cdot D_{tloss}. \cdots\cdots (7)$$

This formula means duty after the degraded D_{PC_V} is $1/\beta$ times greater than the initial duty D_{tloss} and is independent of I_{out}.

On the other hand, if the relative CTR degradation changes from 1 to γ ($0 < \gamma < 1$) in the photo-coupler installed in the current detection circuit, the actual output current increases from I_{out} to $1/\gamma \cdot I_{out}$. So, applied duty after the degraded D_{PC_I} is formulated as

$$D_{PC\_I} = \frac{1}{\varepsilon(1/\gamma \cdot I_{out})} \cdot \frac{V_{out}}{\alpha \cdot V_{in}} = \frac{(R_{load}(1/\gamma \cdot I_{out}) + R_{loss}(1/\gamma \cdot I_{out}))}{R_{load}(1/\gamma \cdot I_{out})} \cdot \frac{V_{out}}{\alpha \cdot V_{in}} = \frac{(R_{load}(1/\gamma \cdot I_{out}) + R_{loss}(1/\gamma \cdot I_{out}))}{R_{load}(1/\gamma \cdot I_{out})} \cdot D_{tloss}. \cdots\cdots (8)$$

If the total loss of SMPS E_{loss} is approximated as

$$E_{loss}(I_{out}) \approx A + B \cdot I_{out} + C \cdot I_{out}^2 \cdots\cdots (9)$$

where A, B and C represent a constant factor represented by the power consumption of the controller chip, a proportional factor represented by switching loss and a square proportional factor represented by resistive loss, respectively.

From formula (9), the apparent loss $E_{loss}(\gamma, I_{out})$ and apparent equivalent resistance $R_{loss}(\gamma, I_{out})$ are formulated as

$$E_{loss}(\gamma, I_{out}) \approx A + B \cdot 1/\gamma \cdot I_{out} + C \cdot 1/\gamma^2 \cdot I_{out}^2 \cdots\cdots (10)$$

and

$$R_{loss}(\gamma, I_{out}) \approx \frac{A + B \cdot 1/\gamma \cdot I_{out} + C \cdot 1/\gamma^2 \cdot I_{out}^2}{1/\gamma^2 \cdot I_{out}^2}. \cdots\cdots (11)$$

From formulas (8) and (11), D_{PC_I} is formulated as

$$D_{PC\_I} \approx \left(1 + \frac{A + B \cdot 1/\gamma \cdot I_{out} + C \cdot 1/\gamma^2 \cdot I_{out}^2}{1/\gamma \cdot I_{out} \cdot V_{out}}\right) \cdot D_{tloss}. \cdots\cdots (12)$$

If I_{out} is great enough, the square proportional factor becomes dominant and formula (12) is formulated as

$$D_{PC\_I} \approx \left(1 + C \cdot \frac{I_{out}}{\gamma \cdot V_{out}}\right) \cdot D_{tloss}. \cdots\cdots (13)$$

Formula (13) means that D_{PC_I} has a linear dependence on I_{out} with a proportional constant of $1/\gamma$ at the higher power region.

As formulated in formulas (7) and (13), the theoretical duties for the degraded converter, D_{PC_V} and D_{PC_I}, have different I_{out} dependence, so we looked at CTR degradation detection for photo-couplers installed in the voltage feedback loop and current detection circuit distinctly by comparing D_{tloss} with $D_{applied}$ or D_{PC_V} and D_{PC_I}.

After this section, ratio between $D_{applied}$ and D_{tloss} notes as *Ratio_duty*.

3. Result and Discussion

3.1 MILS: Model in the Loop Simulation In this section, sensitivity analysis using model in the loop simulation (MILS) using MALTAB/Simulink with PLECS is described. A 500 W full bridge converter, which is a standard

Table 1. Specifications of evaluated converter for MILS* and RCP**

Item	Specification and parameters
Circuit topology	Full bridge converter with synchronous rectifiers
Input voltage	400 V
Output voltage	12 V
Output Current	0 to 41.67 A
Output power	0 to 500 W
Input capacitor	330 μF
Output capacitor	1500 μF x 5
Output inductor	2 μH
Transformer	21:1 turn
Chopper FET	Infineon SPP20N60CFD
Rectifier FET	Fairchild FDP032N08
Switching frequency	100 kHz
Control frequency	100 kHz
ADC resolution	3.3 V full-scale 11bit
AAF cutoff frequency	20 kHz
Crossover frequency	2 kHz
Compensator type	Simple integrator* 3 pole 3 zero (Type 3 equivalent)**
Gain margin	10 dB (designed)
Phase margin	45 degrees (designed)
Controller**	RCP System
PC degradation	Emulated with sense amp gain decrease

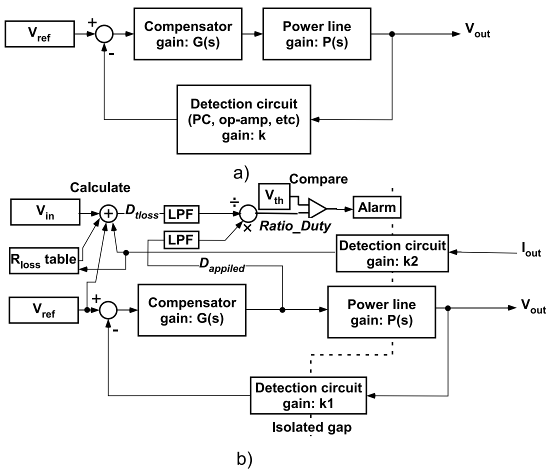

Fig. 4. Block diagrams of a) conventional and b) proposed feedback loops. Comparing applied duty $D_{applied}$ and theoretical Duty D_{tloss} detects both voltage and current CTR degradation

test bed for our failure prediction study [(13)–(15)], is used for evaluation. The converter specification is summarized in Table 1, and is assumed as a second stage power supply unit or PSU for servers†.

Figure 4 shows a block diagram of the a) conventional and b) proposed feedback loops, comparing the I_{out} dependence of applied duty $D_{applied}$ and the theoretical duty D_{tloss} detecting CTR degradation and alerting for failure. The R_{loss} table is defined as a function of I_{out} using a conventional feedback loop in advance of the application of the proposed one.

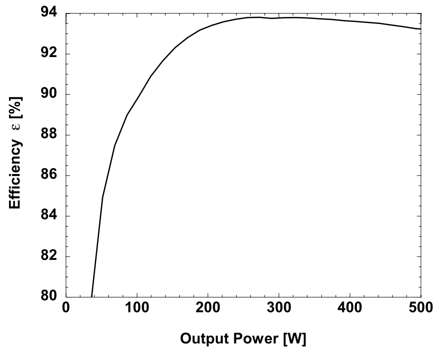

Fig. 5. Efficiency curve of evaluated convertor

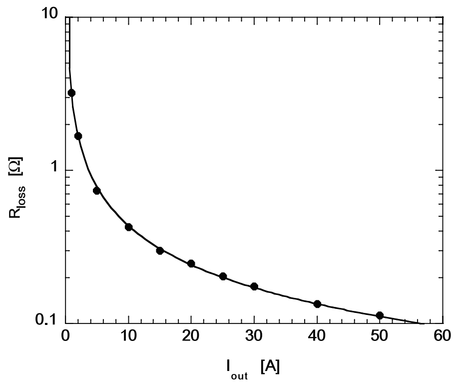

Fig. 6. I_{out} dependence of equivalent resistance R_{loss} for evaluated converter

Figures 5 and 6 show the efficiency curve and relation curve between the efficiency ε and the equivalent resistance R_{loss} for the modeled converter.

Using this R_{tloss}, the I_{out} dependence of *Ratio_Duty* for Voltage detection photo-coupler (Fig. 7) and for Current detection photo-coupler (Fig. 8) at steady state are evaluated. V_{Gain} and I_{Gain} are each decreased by 1% and 10% steps, respectively. At an I_{out} range of over 10 A, the deviation of *Ratio_Duty* for Voltage detection photo-coupler is suppressed at ± 0.5%. An abrupt increase of R_{loss} in the lower current range causes greater deviation in the lower current range. However, as expected from formulas (7) and (13), constant and linear dependences of *Ratio_Duty* for Voltage and Current detection photo-coupler on I_{out} are observed. In the Voltage detection photo-coupler case, the gain decrease ratio is equal to the increasing ratio of D_{PC_V} and a 1% decrease of CTR is sufficiently detectable. For example, in a power supply unit for servers, the output voltage regulation specification is 12 ± 5% and 1% resolution power is high enough for over-voltage detection. On the other hand, the resolution power in the Current detection photo-coupler case is one order lower than the Voltage detection photo-coupler case. A 20% decrease in CTR can cause only a 2 or 3% change in *Ratio_Duty*. This means that this method is difficult to use for calibration of current detection circuits. However, we believe this method is useful in terms of functional safety. Activating emergency fire-fighting equipment may cause severe damage to a datacenter even if the fire does not directly damage the ICT facilities [(18)]. Alarming several tens of percent of over-current can reduce the smoke and fire risk to a power supply.

† 80 PLUS [(17)] silver certified PSU is assumed, second stage DC/DC is installed after first stage power factor correction (PFC) circuit. 80 plus silver certification requires efficiency of 89% @ 230 V_{ac} input, half load, thus around 94%+ efficiencies are required of both the PFC and DC/DC circuit.

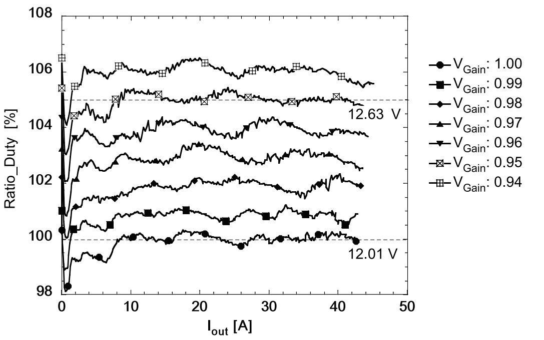

Fig. 7. MILS evaluated I_{out} dependence of *Ratio_Duty* for voltage detection circuit

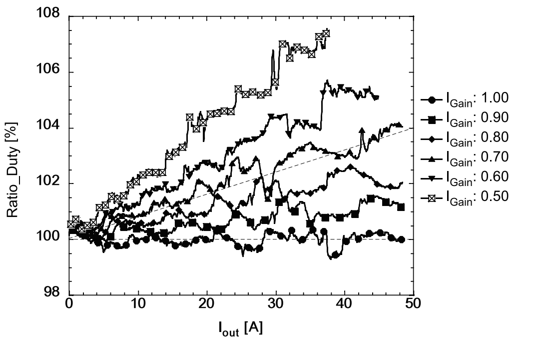

Fig. 8. MILS evaluated I_{out} dependence of *Ratio_Duty* for current detection circuit

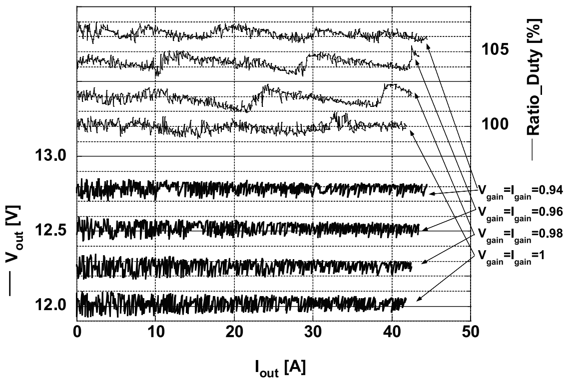

Fig. 9. I_{out} dependence of V_{out} and *Ratio_Duty* when both voltage and current detection photo-coupler degraded at the same time

Usually, CTR degradation occurs very slowly with the order of months or years, checking I_{out} dependence of *Ratio_duty* once a day is enough frequent. So this method is not significant influence on the load of controller MPU.

There is a possibility of both photo-couplers may degraded simultaneously in the same SMPS. Figure 9 shows I_{out} dependence of V_{out} and *Ratio_duty*. As mentioned above, sensitivity of Ratio_Duty for current detection photo-coupler is one order lower than for voltage detection, the effect of current detection photo-coupler degradation is not observed.

To eliminate higher frequency component caused by abrupt load change, sampling frequency for calculating *Ratio_duty* is selectable enough lower than the response frequency of the converter. If the sampling frequency is set as same as sampling frequency of converter control, higher frequency component is reduced by low pass filter (LPF) with lower frequency than response frequency.

How to determine threshold voltage for alarm is significant issue. Two *Racio_Duty* components, for Voltage and Current detection circuit degradation, have different I_{out} dependence. At least two data sets of I_{out} and *Racio_Duty*, this difference is distinguishable. Usually degradation occurs very slowly and these data sets may evaluate one time for a day is enough. 3 and 5% degradation for voltage detection circuit is suitable for first and final alarm for voltage detection. On the other hand, alarm threshold for current detection circuit should be determined in reference with cooling margin of the installed system. Usually about 20% of cooling margin is applied for SMPS installed system, *Racio_Duty* threshold for current detection circuit should be the value corresponding to 15% and 20 % loss increase for full load of system.

When connected load shows suitable load change in normal operation. Changing rotation speed of cooling fan for power supply can be available.

Efficiency drop caused by ambient temperature may cause difference with *Ratio_Duty*. However, ambient temperature dependence of converter efficiency is relatively small. For example, on resistance of On Semiconductor FDP032N08 [19], rectifier FET installed in test bed, changes from 3.8 mΩ to 4.8 mΩ for junction temperature from 50 to 150°C. This is corresponding to 1.6 W loss increase and 0.4% point efficiency drop at I_{out} 40 A. This value is too small for 1% point change of *Ratio_Duty*. Of course, significant efficiency drop caused by SMPS degradation, may be detectable with this method. We think this is future work.

3.2 RCP: Rapid Control Prototyping In this section, we verified the sensitivity of this method by rapid control prototyping (RCP). RCP is described in detail in other papers [11][13]–[15]. RCP has two great advantages for conventional development processes. The first advantage is separating debugging processes in hardware and firmware. Using a sufficiently high-performance control emulator, we can debug the control algorithm without worrying about side effects such as delays in switching timing, code size overflow, incorporation of hand-coding bugs, and so on. These can easily occur in the hand-coding process for the new algorithm. By selecting the controller after algorithm and hardware debugging, we can select the most cost-effective controller with sufficient performance levels. The second advantage is direct monitoring of IO fetched data. The RCP system can evaluate the same IO data sent to the controller, so there is no distortion such as probing problems. Probing analog IO ports can easily cause control instability by noise propagation through probing cables. We can evaluate sensitivity for circuit component degradation and noise immunity of the control circuit directly from the controller fetched data.

Figure 10 shows the difference between measured output current I_{out} and the controller fetched output current $I_{out\_fetched}$. Due to a characteristic of a current transformer installed in the converter circuit, linearity in the lower current region—below 10 A—is degraded. As shown in Fig. 6, the R_{loss} changes rapidly in the below 10 A range, D_{tloss} under the 10 A range is not trusted. The CTR degradation is emulated as gain suppression prior to AD conversion. I_{out} dependence of both *Ratio_dutys* for voltage detection (Fig. 11) and for current detection are evaluated by RCP. Unlike a MILS

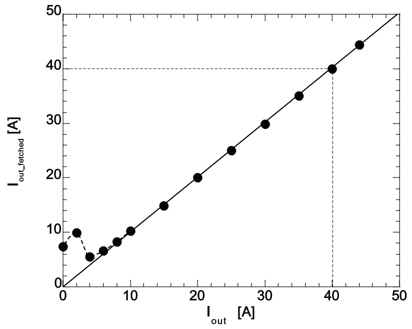

Fig. 10. Difference between measured output current I_{out} and controller fetched output current $I_{out\_fetched}$

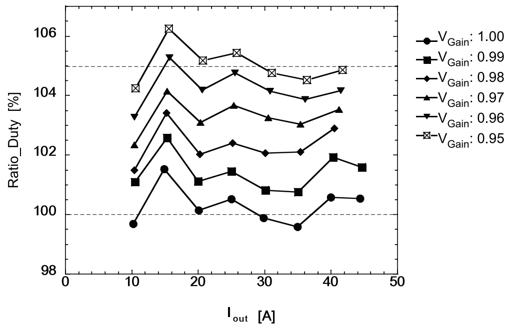

Fig. 11. *Ratio_Duty* for voltage detection photo-coupler degradation measured with RCP

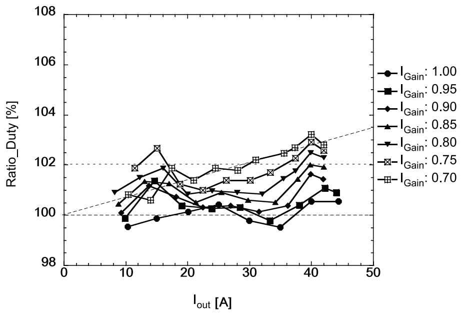

Fig. 12. *Ratio_Duty* for current detection photo-coupler degradation measured with RCP

evaluation, the I_{Gain} decrease is limited to 0.7 and load power is limited to 650 W to avoid damage to the converter. This means 130% over-power, 650 W for 500 W rated SMPS. The cooling fan for SMPS was also enhanced. The accuracy of both *Ratio_duty for* voltage detection degradation (Fig. 11) and *Ratio_duty for* current detection degradation (Fig. 12) are also degraded in the lower current range. Around 1 and 10% CTR resolution power are verified for V_{out} and I_{out}, respectively.

Although *Ratio_duty* for voltage detection degradation varied in ±0.5% range, they have peaks and valleys at I_{out} of 15 A and 35 A. We think they are related to the resolution power of I_{out} in R_{loss} table. In MILS simulation, R_{loss} table is automatically generated in simulation and have much enough resolution for I_{out}. However, in the case of RCP, efficiency curve is measured manually and interpolated to make R_{loss} table. Higher resolution and accuracy may improve accuracy of *Ratio_Duty*, ± 0.5% accuracy is enough for degradation detection/failure detection of photo-coupler. The issue of R_{loss} table accuracy may significant for compensating production variation of photo-coupler. R_{loss} table calibration may be required for each SMPS, however, it also must be determined trade-off between calibration cost and accuracy.

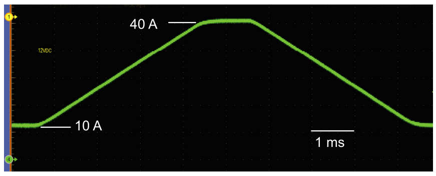

Fig. 13. Current waveform for triangle wave measurement

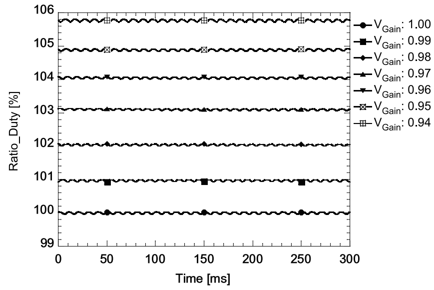

Fig. 14. D_{PC_V}/D_{tloss} for the triangle current waveform with IIT low pass filters

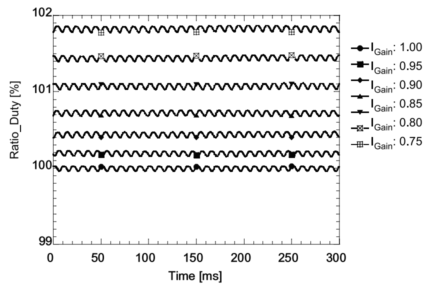

Fig. 15. D_{PC_I}/D_{tloss} for the triangle current waveform with IIT low pass filters

To eliminate the influence of the low accuracy range, enhancing a low pass filter is effective. *Ratio_duty* for voltage detection degradation (Fig. 13) and *Ratio_duty for* current detection degradation (Fig. 14) are evaluated with a triangle wave load. IIT filters with a 3 Hz cut-off frequency are installed both before the D_{tloss} calculation and the $D_{applied}$ comparison. Figure 12 shows the current waveform of the triangle wave load, 100 Hz with an average current of 30 A. Even though the value is inaccurate near the 10 A region, the resolution powers of both voltage and current are higher than 1%.

These methods required at least two IIR filters for D_{tloss} and $D_{applied}$, one division for calculating D_{tloss}, and some comparators for alert thresholds; these are very simple algorithms and easy to implement on low power microprocessors for converter control.

4. Conclusion and Future Work

We have proposed a new online photo-coupler CTR degradation method for digitally-controlled converters. Comparing theoretical and applied duties calculated solely from normally controller fetched current and voltage values, CTR degradation can be evaluated with a resolution power of 1% and 10% for photo-coupler voltage and current detection circuits. The applied duties have different output current dependencies for the voltage and current CTR degradation. Using this difference, both degradations are detected separately. We are now trying to make a prototype for the concept of digitally-controlled SMPS with this failure prediction function, and verifying its effectiveness.

Acknowledgment

The authors extend their thanks to Dr. Tomotake Sasaki of Fujitsu Laboratories LTD., Mr. Hisato Hosoyama and Mr. Atsusi Manabe of Fujitsu Advanced Technology LTD. for their useful comments about RCP and PCG. The authors also wish to gratefully acknowledge the support of Dr. Takeshi Horie, Head of the Computer Systems Laboratory at Fujitsu Laboratories Ltd. who gave us the chance to perform this research. Special thanks to Mr. Kouichi Kumon, member of the board at Fujitsu Laboratories Ltd. who gave us a great deal of support and useful advice.

References

(1) "Basic characteristics and application circuit design of transistor photocouplers", Toshiba, [online], https://toshiba.semicon-storage.com/info/docget.jsp?did=13438, last accessed at May 21th 2017.

(2) "Overvoltage-protection circuit saves the day", Linear Technology, [online], http://www.linear.com/docs/39658, last accessed at May 21th 2017.

(3) "Datasheet of HCNR200 and HCNR201", Avago Technologies, [online], www.avagotech.com/docs/AV02-0886EN, last accessed at May 21th 2017.

(4) "Datasheet of TLP7820", Toshiba, [online], http://toshiba.semicon-storage.com/info/lookup.jsp?pid=TLP7820&region=ncsa&lang=en_us, last accessed at May 21th 2017.

(5) "DOSA standard specification of eighth brick DC/DC converter", [online], http://www.dosapower.com/standards.html, last accessed at May 21th 2017.

(6) IEC60065, [online], https://webstore.iec.ch/publication/494.

(7) "R2A20133DSP datasheet" RENESAS, [online], https://www.renesas.com/en-us/doc/products/linear/r03ds0052ej0401_r2a20133d.pdf, last accessed at May 21th 2017.

(8) J. Schäuffele and T. Zurawka: "Automotive software engineering principles, processes, methods and tools", Warrendale, Pa.: SAE International (2005)

(9) R.K. Jurgen, Ed.: "Automotive Software: PT-127", Warrendale, Pa.: 0000000000000000000000000 SAE International (2006)

(10) J. Krasner: "Comparing embedded design outcomes with and without model-based design", American Technology International", White Paper (2010)

(11) Y. Yonezawa, T. Sasaki, H. Hosoyama, H. Nakao, A. Manabe, J. Kaneko, Y. Nakashima, and T. Maruyama: "Rapid control prototyping for server power supply with high-resolution PWM", in Proc. APEC2015: 2015 the 30th annual IEEE applied power electronics conference and exposition, pp.2635–2641, Charlotte, USA (2015)

(12) T. Sasaki, H. Hosoyama, Y. Yonezawa, A. Manabe, K. Huang, X. Liu, J. Chen, J. Kaneko, and Y. Nakashima: "Production code generation for server power supply controller", in Proc. APEC2015: 2015 the 30thannual IEEE applied power electronics conference and exposition, pp.2656–2663, Charlotte, USA (2015)

(13) H. Nakao, Y. Yonezawa, Y. Nakashima, and F. Kurokawa: "RCP evaluation of electrolytic capacitor degradation for SMPS failure prediction", in Proc. APEC2016: 2016 the 31st annual IEEE applied power electronics conference and exposition, pp.754–758, Long Beach, USA (2016)

(14) H. Nakao, Y. Yonezawa, Y, Nakashima, and F. Kurokawa: "Failure Prediction Using Low Stability Phenomenon of Digitally Controlled SMPS by Electrolytic Capacitor ESR Degradation", in Proc. APEC2017: 2017 the 32st annual IEEE applied power electronics conference and exposition, pp.2323–2328, Tampa, USA (2017)

(15) H. Nakao, Y. Yonezawa, T. Sugawara, Y, Nakashima, and F. Kurokawa: "Online Evaluation Method of Electrolytic Capacitor Degradation for Digitally Controlled SMPS Failure Prediction", IEEE Trans. Power Electron., in press.

(16) A. Elbanhawy: "Is power conversion efficiency running out of steam as a comparison tool?", Proc. INTELEC'05: The 27th International Telecommunication Energy Conference, pp.51–57, Berlin, Germany (2005)

(17) 80 PLUS [Online], http://www.plugloadsolutions.com/80PlusPowerSupplies.aspx, last accessed at May 21th 2017.

(18) B.P. Rawson and K.C. Green: "Inert Gas Data Center Fire Protection and Hard Disk Drive Damage", The Data Center Journal, [Online], http://www.datacenterjournal.com/inert-gas-data-center-fire-protection-and-hard-disk-drive-damage/, Aug. 12 2012, last accessed at May 21th 2017.

(19) "Datasheet of FDP032N08", On semiconductor, [online], http://www.onsemi.com/pub/Collateral/FDP032N08-D.pdf, last accessed at Jan. 12th 2018.

Hiroshi Nakao (Student Member) was born in Chiba Prefecture, Japan in 1964. He received his Master's degree in Physics in 1989 from Tokyo University of Science, Tokyo, Japan. Since September 2015, he has also been pursuing a Doctorate in Electrical Engineering and Computer Science from the Graduate School of Engineering, Nagasaki University, Nagasaki, Japan. Since completing his Master's degree researching the crystal growth of semiconductor thin films, he has been employed at Fujitsu Laboratories, Kanagawa-Ken, Japan (since 1989), and is engaged in a wide range of research fields from semiconductor materials/devices to server power supply systems. Using the original development scheme for digitally-controlled power supplies - model-based design – he and his colleagues are now studying failure prediction of switching mode power supplies.

Yu Yonezawa (Member) was born in Miyagi Prefecture, Japan in 1975. He received his Ph.D. in Functional Materials from Ishinomaki Senshuu University, Ishinomaki, Japan in 2005. He has been employed at Fujitsu Laboratories, Kanagawa-Ken, Japan since 2009. His current research focus includes power supply technologies, especially model-based development technologies of digitally-controlled power supplies.

Takahiko Sugawara (Non-member) was born in Miyagi Prefecture, Japan in 1969. He received his Ph.D. in Engineering from Tohoku University in 1997 following research into giant magnetoresistance in thin films. He has been employed at Fujitsu Laboratories since 1998 and is engaged in research into a read head for a hard disk drive and power supplies for server systems.

Yoshiyasu Nakashima (Member) was born in Nagasaki Prefecture, Japan in 1963. He received his Master's degree in Electronic Engineering from Saga University, Japan in 1989 following a research project on medical electronics. He has been employed at Fujitsu Laboratories since 1989. His current research area is power saving and power supply technologies for server systems.

Fujio Kurokawa (Senior Member) was born in Yamaguchi, Japan, in 1952. He received his B.Sc. in Electronic Engineering from the Fukuoka Institute of Technology, Fukuoka, Japan, in 1976, and his D.Eng. in Electronic Engineering from Osaka Prefecture University, Sakai, Japan, in 1988. Since 1984, he has been with Nagasaki University, Nagasaki, Japan, and is currently a Professor and Head of the Division of Electrical Engineering and Computer Science, Graduate School of Engineering. His research and teaching interests include the areas of digital power, switching power supplies for telecommunications, solar power supply, power plant control, and ion engine control for satellites. Dr. Kurokawa is a Fellow of the Illuminating Engineering Institute of Japan, and also a senior member of the Institute of Electronics, Information and Communication Engineers of Japan, and the Institute of Electrical Engineers of Japan.